Danish Meteorological Institute
Ministry for Climate and Energy

Danish Climate Centre Report 13-04

Removing scattered light in observations of earthshine - tests of three methods

Peter Thejll, Hans Gleisner, Chris Flynn

Colophone

Serial title:
Danish Climate Centre Report 13-04

Title:
Removing scattered light in observations of earthshine - tests of three methods

Subtitle:
Authors:
Peter Thejll, Hans Gleisner, Chris Flynn

Other Contributers:
Responsible Institution:
Danish Meteorological Institute

Language:
English

Keywords:
Data reductions, imaging, scattered light, techniques

Url:
www.dmi.dk/dmi/dkc13-04

ISSN:
1399-1957

ISBN:
978-87-7478-629-0 (online)

Version:
1

Website:
www.dmi.dk

Contents

Colophone 2
1 Dansk resumé **4**
2 Abstract **5**
2.1 Introduction 6
2.2 Methods and Synthetic data 7
2.2.1 Synthetic lunar images 7
2.2.2 The LINEAR sky-extrapolation method 8
2.2.3 The empirical forward method - EFM 8
2.2.4 The full forward method - FFM 9
2.3 Results from tests on synthetic images 9
2.3.1 Results of the LINEAR and LOGARITHMIC methods 9
2.3.2 Results from the EFM method 10
2.3.3 Results from the FFM method 10
2.4 Discussion 11
2.5 Summary and Conclusions 14
3 Previous reports **17**

1. Dansk resumé

Jordens klima styres af strålingsbalancen - balancen imellem indkommende kortbølget sollys og udstrømmende langbølget varmestråling. Balancen påvirkes af jordens reflektivitet - kaldet albedo - og dermed af jordoverfladens reflektivitet, skymængden og mængden af is og sne. Denne albedo kan måles fra rummet med satelitter, men skal måles meget nøjagtigt og på en varig måde således at data kan bruges i klimastudier i fremtiden. Sålænge der ikke findes et alternativ til satelitter vil man være usikker på hvor gode de opmålte data fra rummet er. Derfor er der igangsat et målekesperiment hvormed jordens albedo måles indirekte, men uafhængigt af satelitterne. Systemet, opbygget af Danmarks Klimacenter ved DMI og Lunds Observatorium, på basis af en VINNOVA bevilling på 5 mio SEK, går ud på at observere Månen fra jordoverfladen. Månen opfanger jo det lys der kastes ud i rummet fra Jorden. Nøjagtige målinger af Månens mørke sides lysstyrke kan bidrage til dannelsen af et uafhængigt datasæt for jordens albedo. Dette kræver meget nøjagtig fratrækkelse af det spredte lys der lander på den mørke side af Månen og som kommer fra den lyse side. Denne rapport beskriver tre metoder til at fjerne det spredte lys og er baseret på analyser af kunstige billeder af Månen skabt således at vi kender svaret og derfor kan vurdere metodernes effektivitet.

2. Abstract

Earth's climate is governed by the radiative balance, and this in turn is governed by the reflective properties of Earth - its atmosphere (clouds, haze) and its surface (deserts, snow and ice, oceans). The reflectivity - or albedo - of these surfaces can be measured from space using satellites, but as long as the satellites are the only method for measuring albedo we will not know how good the data are - and this is a serious problem for future climate studies based on satellite data. An independent method is therefore called for. Use of so-called earthshine observations can help in this respect. Earthshine is the light that falls on the Moon from Earth - it can be photometrically characterized by observing the dark side of the Moon using small telescopes on Earth. A necessary step is the removal of scattered light from the bright side of the Moon which lands on the dark side. In this report we document the test of three methods for removing scattered light. We apply the methods to images generated synthetically so that we 'know the answer' and therefore can evaluate the methods' abilities to remove scattered light.

2.1 Introduction

Terrestrial albedo is a key factor in Earth's radiative balance and thus in climate research. Albedo changes as the climate system changes – cloudiness, land-use changes, extent of ice and snow on sea and land, whitecaps on windy oceans, biological activity, aerosol load and so on all depend on the state of the climate system - but induced changes in albedo may also *cause* climate change. Simple energy-balance model considerations suggest that a 1% change in albedo is roughly equivalent to a mean global temperature change of 0.5 K. Feedback processes in the climate system are certainly expected to modify that simplistic picture: but it is evident that precisions on the terrestrial albedo data in the sub-1% range are required to empirically consider the role of albedo in climate change - whether passive or active.

Prior to the satellite era, knowledge on the terrestrial albedo was very uncertain and not until the first space-based determinations of the Earth's radiation budget – those of the Nimbus-6 and 7 satellites – was it firmly established that values of the albedo at short wavelengths is close to 0.3 (Stephens et al. 1981). The result was based on measurements from satellites in low-Earth orbit, which were hampered by temporal sampling problems. Since then, such observations have been supplemented by observations from geostationary orbit. While the instruments on Earth-observing satellites have gained in sophistication and precision, the GERB instrument of the geostationary MSG2 satellites is only required to be 1% accurate at visual wavelengths following laboratory calibrations (Johannes & Mueller 1997). Once in space calibration is based on observation of terrestrial reference surfaces (e.g. salt lakes) or the Moon. In the latter case the Moon is imaged from the satellite and calibrated against a database of lunar irradiance values for different phases of the Moon (Stone 2008). In principle, it should thus be possible to maintain instrument accuracies in the short wavelengths near the 1% level, while precision is better than that.

An alternative method, complementary to current satellite based observational systems, is to measure the ratio of the intensity of the Moon's dark side (DS; illuminated only by earthshine) to that of the bright side (BS; illuminated also by sunshine). The BS intensity is proportional to the solar irradiance while the DS intensity is proportional to the fraction of the solar irradiance reflected off the Earth in the direction of the Moon. Hence, the BS to DS ratio is proportional to Earth's albedo, where the proportionality constant depends only on geometry and factors related to the reflective properties of the Moon. To acquire global albedo information from lunar observations a global network of automated Moon telescopes is needed. At present at least four of these instruments exists – one at Big Bear Solar Observatory in California, one on Tenerife in the Canary islands and one in Crimea (Goode et al. 2010) and now ours at the Mauna Loa Observatory on Hawaii. Additional instruments are needed in Eastern Asia or Australia.

The relative-photometry method described above incorporates *common-mode rejection* of some of the factors that confound absolute-intensity observations: effects of time-varying atmospheric transparency, instrument sensitivity variability, and variations of the solar irradiance. It has been suggested (Goode et al. (2001) and Pallé et al. (2009)) that such albedo observations can potentially reach higher precision than traditional satellite based observations. However, the advantages of common-mode rejection only applies to those effects – instrumental or atmospheric – that remove photons from the path. Scattering of photons from the BS into the DS on the imaging device still gives rise to errors. Hence, the main technological challenge involved in designing equipment for this type of measurements is to minimize the amount of scattered light, and one of the major challenges in the photometric analysis of the images is to properly remove the effects of the remaining light.

This report analyses methods for removing scattered light by using synthetic images for which we 'know the answer' and therefore can evaluate and intercompare the methods.

2.2 Methods and Synthetic data

We first discuss our method for constructing synthetic lunar images. Then we discuss existing and new methods for removing scattered light from images of the Moon. The new methods are based on a forward modelling paradigm.

2.2.1 Synthetic lunar images

Synthetic lunar images are used for assessment of the methods for removing scattered light in the images. These synthetic images are produced by a *lunar radiance model* that simulates the appearance of the Moon in a CCD image. The model accounts for the viewing geometry and uses broad-band bi-directional reflection functions (BRDFs) to describe how sunshine is scattered off the lunar surface. The scattering properties depend on the selenographic latitude and longitude – i.e. location on the Moon – and account for the different reflection properties of the lunar maria and highland regions. The result of the simulation is an 'ideal' image of the Moon unaffected by scattering of light in the atmosphere or instrument.

The components of the lunar radiance model are:

- a geometrical description of the Earth-Moon-observer system
- a photometric description of the lunar light-scattering properties
- a simplistic photometric description of the terrestrial light-scattering properties
- an algorithm to ray-trace from the individual CCD pixels to the surface on the Moon

The geometrical description is taken from an ephemeris describing the positions and rotations of Earth and Moon as a function of time. The geometric description includes the observer's position, the lunar librations, and the distance and direction of the Sun from the Earth-Moon system.

The BRDFs describe the probability that an incident photon is scattered in a certain direction as a function of angle of incidence, angle of reflection, and phase angle. The formulation of the BRDF follows Hapke (1963) and Hapke (1993), and the BRDF is normalized to give an albedo roughly similar to that measured in the 750 nm band by the UV/VIS camera on-board the Clementine mission (Robinson & Riner 2005).

The role of the model Earth in the present setup is to illuminate the Moon with ES. The illumination must be of the right order of magnitude for the DS to BS intensity ratio to be realistic. This can be accomplished by a simple Lambertian sphere Earth-model with a uniform single-scattering albedo (SSA). To generate temporal albedo variations, an optional Earth albedo model incorporating land, ice, and ocean reflections, and a realistic cloud distribution, is available (Ford et al. 2001).

The lunar images are produced by a simple form of ray tracing. Each pixel on the imaging device collects light from a certain solid angle in a certain direction. This direction is traced to the surface of the Moon. From the computed selenographic latitude and longitude, and knowing the angle of incidence of the sunshine and ES, and the phase angle at the Moon, we can compute the light scattered in the direction of the observer. This is done for each individual pixel leading to the

buildup of an image. An advantage of this simple ray-tracing algorithm is that it gives the correct stereo-graphic projection as a result of the finite Moon-observer distance, without explicitly computing the projection effects. Scene models where the Earth is rendered have been described, for realistic image rendering purposes in the animated-motion picture industry (Jensen et al. 2001), for exoplanet investigations (Oakley & Cash 2009) and recently (Yu et al. 2011) for a space-based ES instrument.

2.2.2 The LINEAR sky-extrapolation method

The BBSO group performing observations of ES Goode et al. (2001) pioneered a method for compensating for scattered light in images of the Moon based on linear extrapolation of the scattered light intensity on the sky. It was noticed that the intensity follows an almost linear dependency on the distance to the lunar disk centre: with a regression estimating the relationship between intensity and radial distance a method was devised for extrapolating onto the lunar disk and subtracting scattered light there.

Calling the above method 'LINEAR' from now on, we will also consider the 'LOGARITHMIC' method: It is the same as LINEAR but works on logarithms of images.

2.2.3 The empirical forward method - EFM

We have also two forward modelling methods based on numerically replicating the process that causes the Moon to be recorded as a blurred and noisy object. After a replica image has been fitted it can be subtracted from the observed image and yield information on the unblurred image.

In the Empirical Forward Model (EFM) we use the bright part of the observed image as a model of the source of the scattered light. Convolving that spatial source with trial flux-conserving PSFs we can iteratively adjust model parameters in the PSF until a good match is found between the sky part of the observed image and the trial synthetic images.

The choices of which part of the image to use as source and which part to use for model fitting influences the results, so testing is in order - and we do so based on synthetic lunar images where the DS intensity is known. As source we choose that part of the observed image where the intensity is above some fixed fraction of the maximum intensity - e.g. 1/75th. This is an arbitrary choice so we experiment to see which value gives good results - setting it too low means that the DS is being included in the model of the source which implies that that part will be removed at the subtraction stage - as the DS increases in relative intensity as the New Moon is approached the choice of the cut-off sets which part of the lunar cycle you can access with the method.

We have found that the difference between modelling the BS source as those pixels with intensity above one 75th of the maximum BS intensity on the one hand, and modelling the source as all pixels that are sun-lit on the other, corresponds to a difference in the halo intensity at the DS reference patch of from 0.01 percent up to a few tenths of a percent, when the resulting model halos are normalized to the same value at maximum. The influence of the choice of source model is even less when we consider the effect of subtracting the *best-fitting* halo, and we shall use the 1/75th rule for building the model source from now on.

We fit the EFM to the sky around the lunar disc, or parts thereof: The minimization requires adjusting three parameters - one equivalent to requiring flux conservation, one equivalent to a pedestal or offset in the image and one parameter (α) setting the width of the PSF. These can be found by using a conventional numerical minimization, or in a grid search with sufficiently small

steps. Typically, the image scaling parameter is linked to the choice of the others and can be found algebraically.

The forward modelling involves the convolution of images with extended PSFs - this is done by multiplication in the frequency domain followed by inverse transformation. Since the PSFs have extended wings we need to 'pad' the images to avoid edge-effects during the FFT based folding - we have found it sufficient to lay them out in a 3×3 grid of same-size empty images.

2.2.4 The full forward method - FFM

The above EFM method yields scattered-light corrected information on the intensity of the DS. Such data still need to be further reduced to yield terrestrial albedo information, as is done by the BBSO team (e.g Qiu et al. 2003). As an alternative, we introduce here the full forward model ('FFM') method in which a model of the Earth and its reflective properties is allowed to set the ES intensity - in this way the various reduction steps used for inverting conventionally observed ES are subsumed into the modelling of the reflection of light at the Earth; a best fitting model is determined and directly yields an estimate of the terrestrial albedo. The fitting of this model to the observations is done on sky as well as on the lunar disc: Again we have two parameters that correspond to flux conservation and matching the sky level, and a third parameter still describes the PSF, but now in addition we have several other parameters or model-choices that can be determined - these describe the terrestrial albedo model.

We present a test of the FFM next, based on synthetic images incorporating an offset, a scaling, a width parameter for the PSF and a terrestrial albedo. The synthetic images are calculated with the system described in section 2.2.1, and appropriate amounts of Poisson noise is introduced. The test proceeds by setting up a series of synthetic images and two auxiliary images for the same phases but where one has been calculated for albedo 0.0 and the other for albedo 1.0. By scaling these two images linearly we enable a non-linear least squares minimization method – MPFIT2DFUN (Markwardt 2009) – to not only find the offset and the PSF parameter, but also, directly, the terrestrial albedo. The image factor is found by imposing flux-conservation between the synthetic realistic image and the fitting routines trial images which depend on the offset, the PSF parameter and the synthetic image illumination (i.e. the ES). The method is set up to minimize the relative root mean square error (RMSE) over the entire image - sky and lunar disc, BS and DS. Individual pixel weights are based on $\frac{1}{\sigma}$ where σ is given by Poisson statistics.

2.3 Results from tests on synthetic images

About a month's worth of realistic but synthetic images were generated at 9 hour intervals, resulting in 83 images, in order to represent all observing conditions. Each of these were made with realistic levels of Poisson noise and blurring, and a realistic maximum exposure level of 55000. The blurring was performed using a power-law PSF based on an empirical profile extended linearly in log-log space; this PSF was then raised to a fixed power. The combined effect of using the empirical power-law and the exponentiation was that of a power law with power near -2.9, corresponding to a clear night with most of the PSF due to telescopic elements.

The images were produced in two sets - one consisting of 83 single images and the other consisting of averages of 100 images, to simulate the effect of the CoAdd method. Each of the images in each set were reduced for scattered light using the above methods.

2.3.1 Results of the LINEAR and LOGARITHMIC methods

We implemented the LINEAR method by closely following Qiu et al. (2003). We tested whether a linear least squares or a least absolute deviation regression works best - very little difference was found. We use the least squares method here because that choice enables a simple evaluation of the goodness of fit. When the regression was deemed 'good' by the formal quality of the fit it was used to extrapolate the regression onto the lunar disk all the way to the disc centre and the extrapolated light subtracted inside the relevant cone. We noted that the data are a little inter-dependent - the estimates of the errors on the data enter into the estimation of the goodness of fit as does the number of points, but few of the regressions seemed to test out as being good - the required p level was rarely reached. We overcame this problem by lowering the parameter that gives the number of independent points from the actual number of points to one third of that: this is consistent with some moderate degree of serial correlation in the residuals - perhaps due to the halo not being quite linear after all, and some curvature noted near the disk rim.

After cleaning the images the DS intensity was extracted from 21×21 pixel patches situated at 2/3rds and 4/5ths of the radius from the disk centre at the same row as the center of gravity of the light, on the DS. The same boxes were measured in the known synthetic images, and the two values compared. Figure 2.1 shows the results as a function of lunar phase. Note that it is in practise very difficult to observe the Moon for any length of time at lunar phases below about 30 degrees - the proximity to the Sun sets the limit,

We see that results with small errors are available only for a narrow range of lunar phases - e.g. less than 40 or 50 degrees. Only for α=-2.88 and high SNR can the methods reach up to phases of 60 or 70 degrees. We see in general that the LOGARITHMIC method is somewhat better than the LINEAR, and that best results are found close to the rim, as expected. We also see an asymmetry - as the lunar phase passed Half Moon the analysis switched to the other side of the lunar disk where an area of different lunar albedo was in the box. These results suggest that application of the LOGARITHMIC method can contribute to better scattered-light removal in the sky-extrapolation framework. In addition, we note the prevalence of a strong bias - for large lunar phases both linear and logarithmic images have increasing levels of residual scattered light with increasing lunar phase.

2.3.2 Results from the EFM method

Figure 2.2 shows results from the test of the EFM method. Two values of α were used, and stacks of 100 images were simulated. We see that for a narrow PSF (α=-2.88) it is possible to determine the DS intensity to better than 1% for lunar phases out to about 100 degrees from New Moon, but that for broader PSFs (ie on lower-quality nights) the error in DS determination is generally at the several-percent level. The Figure shows absolute values of errors for display purposes: There was little bias in the α=-2.88 results with errors scattered around 0, while bias was present for the α=-2.56 case - most errors had the same sign.

2.3.3 Results from the FFM method

Figure 2.3 shows the results for the FFM - we extract the terrestrial albedo directly (shown), as well as the sky offset, flux factor and α (not shown). For single images results are within $\pm0.2\%$ from the known value for lunar phases up to 60 to 80 degrees, depending on the PSF width. Bias, is present but small. When 100 images are coadded the method improves markedly - bias is almost gone and acceptable results are obtained for phases up to ±110 degrees. Due to issues related to difficulties in realistically estimating the number of degrees of freedom in the data we do not show the fitting methods' formal estimates of uncertainties, as these are probably underestimated. Instead we

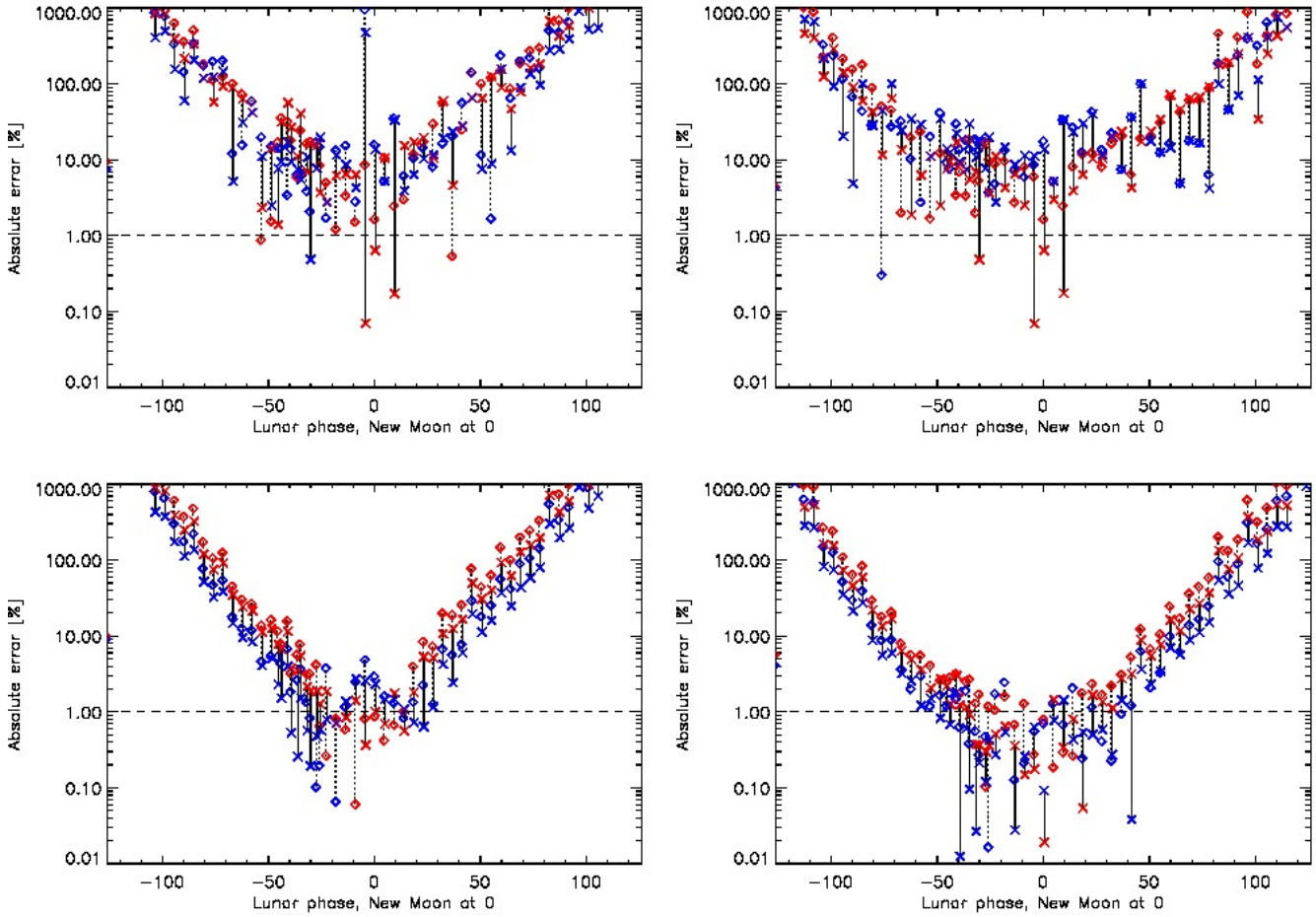

Figure 2.1: Test of LINEAR (red symbols) and LOGARITHMIC method (blue) on realistic synthetic images. Absolute percentage errors, calculated from corrected images and the known ideal images are shown. Upper row: A single image with α=-2.56 (left) and -2.88 (right). Crosses show the results at 4/5ths of the disk radius from disk center and diamonds are for 2/3rds from disk centre. Lower row: 100 realistic images co-added. The abscissa shows lunar phase in degrees relative to New Moon at 0. Note that phases from about -40 to +40 degrees are in practise unobservable. The ordinate shows absolute values only in order to accommodate a few negative percentage errors near lunar phase 0: The sense of the error is primarily such that corrected images carry more flux than is present in the ideal images.

estimate the errors using Monte Carlo simulations. One standard deviation intervals for the fits are estimated by performing Monte Carlo simulations at two characteristic lunar phases: The fit was estimated 100 times using new realizations of the Poisson noise - this gives a distribution in the fitted albedo, for instance, which can be used to realistically discuss the errors on the FFM as a function of lunar phase. Table 2.1 shows the results.

2.4 Discussion

We have seen the LINEAR and LOGARITHMIC methods work well on synthetic test images in a narrow range of lunar phases. We have seen how the LOGARITHMIC extends the powers of the LINEAR method, and we have seen the effect of working on high SNR data. We also saw a strong bias for large lunar phases: This is not unexpected as the ES intensity drops as lunar phase increases

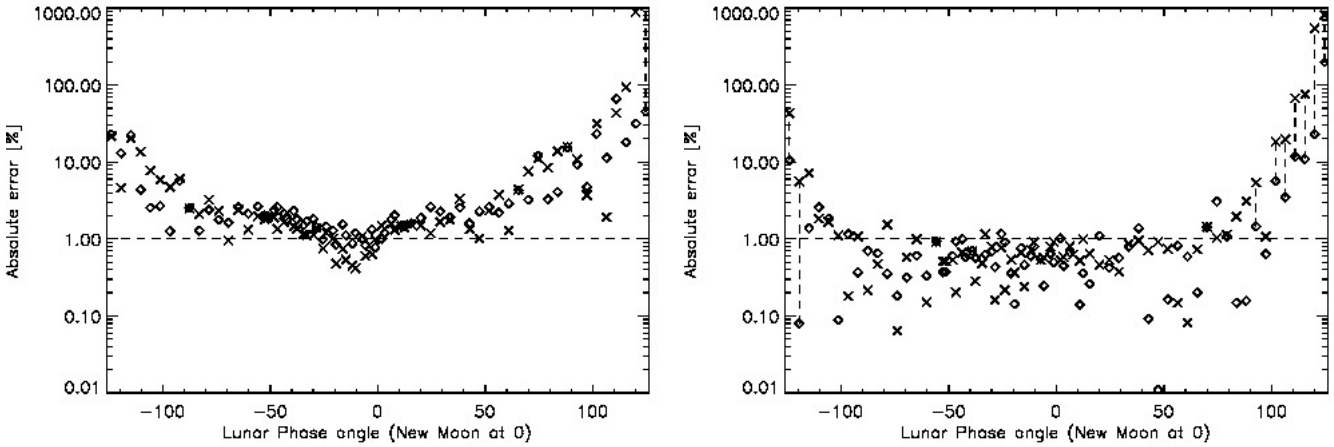

Figure 2.2: Empirical forward method tested on synthetic lunar images. At left is the test using synthetic images with α=-2.56 and at right for -2.88. Stacks of 100 coadded images were simulated for every 9 hours in a lunar month. The lunar phase is shown in degrees using New Moon as phase 0. The error is the difference, expressed in percent, between the actual DS intensity and the value in images cleaned with the EFM method. Crosses indicate values from a patch on the image at 4/5ths of the radius from disk center towards the DS rim, and diamonds indicate values in a box at 2/3rds radius from the disk centre. Absolute values of errors are shown.

Table 2.1: Estimates of FFM method fitting error on albedo, from Monte Carlo simulations and synthetic lunar images. For two lunar phases and two choices of the number of images to stack, 100 Monte Carlo realizations of the Poisson noise in the synthetic image were produced and the best fitting FFM model found for each. The resulting 100 values of the albedo were placed in a histogram and the standard deviation and the median value bias extracted. Lunar phase is 0 at New Moon. Emphasized with bold are cases where both uncertainty and accuracy is better than 0.1%.

Lunar phase	No. of im.	α	Δalbedo	Median bias
-36.7	1	-2.56	0.122%	-0.225%
-36.7	100	-2.56	**0.013**%	**0.049**%
-36.7	1	-2.88	0.098%	-0.178%
-36.7	100	-2.88	**0.0**%	**0.058**%
86.1	1	-2.56	0.66 %	-0.59%
86.1	100	-2.56	**0.08**%	**0.010**%
86.1	1	-2.88	0.37 %	-0.34%
86.1	100	-2.88	**0.04**%	**0.012**%

- the proximity of all DS areas to the wings of the BS halo also increases with lunar phase: Essentially the LINEAR method cannot cope with the halo when it is strong and the reference patch is close to it. We understand the PSF as a power-law entity and understand why these methods have limited applicability for large lunar phases: A power law is first of all not linear with distance to the center; only approximately so at large distances and narrow radial intervals - secondly, the LOGARITHMIC method also fails at a slightly larger lunar phase because the method is applied in lin-log space - and a power law is only perfectly linear in log-log space.

The FFM method seems to be the best method of those analyzed: It yields very accurate and precise estimates of the terrestrial albedo. It does so by utilizing virtually all pixels in the image, which leads to a higher quality fit. When DS intensities are reported we have a contribution from spatial variance in the lunar image considered - this increases the reported error: For the tests considered in this

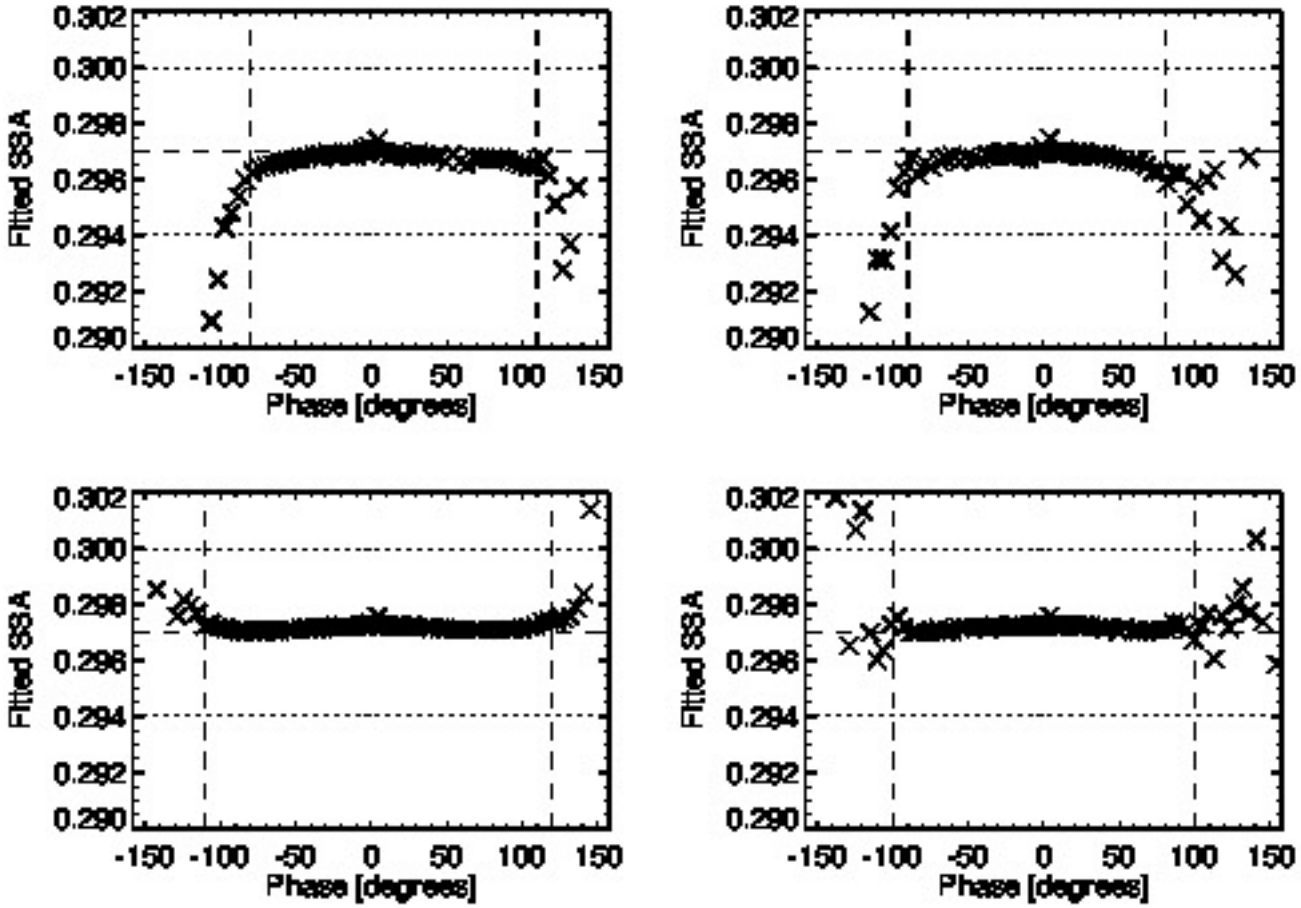

Figure 2.3: Full forward method tested on synthetic lunar images. Shown is the value for single scattering albedo retrieved by fitting models to images generated with known settings of the terrestrial albedo. In the top row are results from single images, against lunar phase: New Moon is at phase zero. In the bottom row are results from fitting images that each were the result of co-adding 100 images. The left column is for $\alpha = -2.56$, the PSF parameter which determines the width. In the right column α=-2.88. In all tests the single scattering albedo on the Lambertian-sphere model Earth was 0.297 which is shown as the dashed line. Dotted lines are the 1% limits. Dashed vertical lines show where the results seem to break down and become too noisy.

report this is a factor for the EFM method where different levels of spatial smoothing in the synthetic observed image and the ideal source are present. The size of the RMSE bias in Figure 2.2 is therefore somewhat higher than the actual model-fit error. The smoothness of the albedo results in Figure 2.3 is impressive, especially compared to the scatter seen for fitted intensities in the other methods' Figures. We ascribe this smoothness to the fact that the FFM extracts a global property from the image, using all the pixels present, while the other methods extract intensities from necessarily rather small areas on the lunar disc. Also, because we are testing in an artificial setting - where we know the general form of the PSF used to make simulated images - the results are overly good - real images have problems we do not model, and results on real images (where, somehow, we knew the properties so that a test was possible) would be less optimistic.

Another factor explains the performance failure of the LINEAR method at large lunar phases - we do not use an internal occulter and therefore the halo around the BS is present in all our images. The BBSO team has available a separate mechanism that inserts a solid knife edge as an occulter of the

BS in the prime focus of their telescope. We speculate, but have seen no published evidence, that the presence of the BBSO-system knife-edge not only reduces the amount of light let into the lower parts of the optical system, but also stops a bright halo being formed in the parts of the optical system between the knife and the CCD. We can conceive of no role for the occulting knife-edge, apart from ghost images (reflections between the internal optics and the back of e.g. the primary objective) and diffuse scattering mentioned above, to reduce the formation of a BS halo if this is generated by the atmosphere (as suggested by Goode et al. 2010) or the first passage of light through the main objective. Careful analysis of ray-tracing experiments through a slightly scattering set of secondary optics may be able to cast light on this question, but is beyond the scope of the present investigation. Unquestionably, the BBSO knife-edge reduces internal diffuse reflections after the prime focus.

The LINEAR and LOGARITHMIC methods work directly on observed images and basically only need tobe told the disk centre coordinates and the radius. The EFM is even easier to use as it requires only an observed image as input. It does, however, require that a choice is made of which BS pixels play the role of source. The EFM method has the advantage that the actual distribution of light on the BS is at hand - in the FFM we have to use a model for this, so we are dependent on how good our lunar reflectance model is.

The FFM models the entire image but requires that the lunar model image is centred and has the right shape and size. Our synthetic model software takes care of the geometric scaling, but centring on the observed image is required.

We have investigated the correction for scattered light using a number of methods. These necessarily involve some choices about how to fit the data in practice. We discuss now some of these choices, the effects they might have, and ideas for further study. In the LINEAR and LOGARITHMIC methods the lunar disk and the sky outside is divided into cones: The width of these cones and their point of convergence are arbitrary choices. We chose the width and the origin of the cones to follow Qiu et al. (2003). Other choices of cone width are certainly possible and it might be useful to start the cones from the BS instead of the centre of the disc. Because the PSF is centrally dominated, although it has wide wings, much of the DS-sky light just off the lunar disk originates in the disk itself and is overlain by the tail of scattered light from the BS. By going too close to the edge of the disk a small chance of introducing a bias by including the 'upturn' exists - one should therefore try to avoid the pixels closest to the Moon. We exclude the pixels nearer than 7 pixels from the rim. In the EFM an important choice is made when positioning the mask that excludes the lunar disc. It should also start off the lunar disc. We start it 16 pixels off the disk rim. Centring of that mask on the lunar disc, and automatically determining the lunar disc radius affects the quality of the subsequent fit, and we want to return to this issue in future work. At present the lunar rim is detected using edge detection techniques on histogram equalized images. Sobel and Laplacian filters (Langford et al. 2009) were tested and were found to perform similarly on real images. The FFM method has no mask to align but the synthetic image used must be aligned with the observed image: The EFM requires a choice of which pixels to use as the 'source'. Both the EFM and the FFM furthermore depend on an offset that is added to images to avoid negative- and zero-valued pixels. Since the *relative* error is minimized the choice of offset influences the objective function to minimize. We have briefly investigated the effect of this on results using synthetic images and find that the best-fit DS/BS ratio does depend on the offset choice. The effect has the nature of a small bias which is a few percent for single images but decreases to the sub-1% level when 100 images are co-added. This implies a biasing dependency on noise in the fitting method.

2.5 Summary and Conclusions

We summarize our synthetic-images based test procedures in Table 2.2. Our extensive tests in this report have confirmed the error levels for the LINEAR method described in publications – e.g. Qiu et al. (2003) and Goode et al. (2010). We have shown that without further corrections of the residual scattered light the LINEAR method will always be biased towards too high a DS intensity. We suggest that the LOGARITHMIC method can ameliorate these effects.

We show that the various flavours of forward modelling methods have the potential to produce more precise and less biased ES intensity data for a wider range of lunar phases, up to about 120 degrees from New Moon in the best case. The FFM method even provides high quality terrestrial albedo values directly without further processing - on single images the uncertainty and the bias is near the stated goal of 0.1%, for lunar phases below 40-50 degrees, while these levels triple if 90 degrees of phase is considered. If we stack 100 images the test is able to achieve very low uncertainty and bias even at 90-110 degrees of phase, showing the effect of the SNR on the fitting method.

Finally, real images are more complex than our simplistic synthetic images and data quality issues not discussed in this report come into play: we are encouraged, however, that stacking of images and forward modelling and fitting of observed images reaches the necessary goals during synthetic testing. In combination with an occulting device that lowers the levels of scattered light inside the telescope, and probably helps eliminate part of the halo around the DS, we expect further improvements in quality of results.

References

Ford, E. B., Seager, S., & Turner, E. L. 2001, Nature, 412, 885

Goode, P. R., Qiu, J., Yurchyshyn, V., et al. 2001, Geophysical Research Letters, 28, 1671

Goode, P. R., Shoumko, S., Pallé, E., & Montañés-Rodríguez, P. 2010, Advances in Astronomy, 2010

Hapke, B. 1993, Theory of reflectance and emittance spectroscopy (Cambridge, UK: Cambridge University Press)

Hapke, B. W. 1963, Journal of Geophysical Research, 68, 4571

Jensen, H. W., Durand, F., Dorsey, J., et al. 2001, in Proceedings of the 28th annual conference on Computer graphics and interactive techniques, SIGGRAPH '01 (New York, NY, USA: ACM), 399–408

Johannes & Mueller. 1997, Advances in Space Research, 19, 1307

Langford, S. V., B. Wyithe, J. S., & Turner, E. L. 2009, Astrobiology, 9, 305

Markwardt, C. B. 2009, in Astronomical Society of the Pacific Conference Series, Vol. 411, Astronomical Data Analysis Software and Systems XVIII, ed. D. A. Bohlender, D. Durand, & P. Dowler, 251

Oakley, P. H. H. & Cash, W. 2009, Astrophysical Journal, 700, 1428

Pallé, E., Goode, P. R., & Montañés-Rodríguez, P. 2009, Journal of Geophysical Research (Atmospheres), 114, D00D03

Table 2.2: Summary of tests of methods to remove scattered-light, based on synthetic image analysis and modelling.

Method name	Description	Pros	Cons
LINEAR	Subtraction of scattered light, extrapolated onto the lunar disk from the sky brightness. Based on linear images. Corrected DS **intensities as output**. Performance improves towards sky edge of the DS. Co-adding many images reduces noise. Works best near New Moon. Can yield errors below 1% up to 40 degrees from New Moon, in best case.	Simple, entirely empirical.	Increasing bias as phase grows. Terrestrial reflectance model needed to convert earthshine intensities to terrestrial albedo.
LOG	Like LINEAR but is applied to logarithms of images. Corrected DS **intensities as output**.	Outperforms LINEAR by another 10 degrees of phase in high SNR images.	Terrestrial reflectance model required.
EFM	Forward modelling and fitting of model image to the sky part of the observed image. Uses bright parts of the observed image as a source term for calculating the model image. Data on the DS intensity is extracted from the difference between the observed image and the best-fitting model image. Corrected DS **intensities as output**.	Works from observed images, avoiding alignment issues and reflectance modelling.	Choice of source region required. Computationally intensive. Terrestrial reflectance model required.
FFM	Forward modelling of entire Moon based on synthetic images of the Moon exposed to ES from a model Earth. Terrestrial **albedo directly as output**.	Can produce albedo data to +/- 90 degrees of lunar phase from single images. +/- 120 from 100-image stack of images. Bias is $\leq$1/5% and the scatter is $\leq$.1 %. For 100 co-added images the bias and scatter is much smaller.	Lunar and terrestrial reflectance model required. Computationally intensive.

Qiu, J., Goode, P. R., Pallé, E., et al. 2003, Journal of Geophysical Research (Atmospheres), 108, 4709

Robinson, M. & Riner, M. 2005, Journal of Earth System Science, 114, 669

Stephens, G. L., Campbell, G. G., & Vonder Haar, T. H. 1981, Journal of Geophysical Research, 86, 9739

Stone, T. C. 2008, in Society of Photo-Optical Instrumentation Engineers (SPIE) Conference Series, Vol. 7081, Society of Photo-Optical Instrumentation Engineers (SPIE) Conference Series

Yu, J., Ryu, D.-O., Ahn, S.-H., & Kim, S.-W. 2011, in Society of Photo-Optical Instrumentation Engineers (SPIE) Conference Series, Vol. 8146, Society of Photo-Optical Instrumentation Engineers (SPIE) Conference Series

3. Previous reports

Previous reports from the Danish Meteorological Institute can be found on:
http://www.dmi.dk/dmi/dmi-publikationer.htm